

# A SIMPLIFIED TECHNIQUE FOR SHAKEDOWN LIMIT LOAD DETERMINATION OF A LARGE SQUARE PLATE WITH A HOLE UNDER CYCLIC BIAXIAL LOADING

**Hany F. Abdalla**  
 Dept. of Mechanical Design  
 and Production  
 Faculty of Engineering,  
 Cairo University, Egypt  
 hany\_f@aucegypt.edu  
 Fax: (202) 795-7565

**Mohammad M. Megahed**  
 Professor of Solid Mechanics  
 Dept. of Mechanical Design and Production  
 Faculty of Engineering, Cairo University, Egypt  
 Vice Dean for Academic and Student Affairs  
 mmegahed47@yahoo.com  
 Fax: (202) 570-3620

**Maher Y. A. Younan**  
 Professor of Mechanics and Design  
 Chair, Mechanical Engineering  
 Dept.  
 The American University in Cairo  
 myounan@aucegypt.edu  
 Fax: (202) 795-7565

## ABSTRACT

A simplified technique for determining the shakedown limit load of a structure was previously developed and successfully applied to benchmark shakedown problems involving uniaxial states of stress [1]. In this paper, the simplified technique is further developed to handle cyclic biaxial loading resulting in multi-axial states of stress within the plate. Two material models are adopted namely: an elastic-linear strain hardening material model obeying the kinematic hardening (KH) rule and an elastic-perfectly-plastic (EPP) material model. The simplified technique utilizes the finite element (FE) method and employs small displacement formulation to determine the shakedown limit load without performing lengthy time consuming full elastic-plastic cyclic loading FE simulations or conventional iterative elastic techniques. The simplified technique is utilized to generate the shakedown domain for the problem of a large square plate with a small central hole subjected to cyclic biaxial tension along its edges. The outcomes of the simplified technique showed very good correlation with the results of analytical solutions as well as full elastic-plastic cyclic loading FE simulations. Material hardening showed no effect on the shakedown limit load of the plate in comparison to employing EPP material.

## INTRODUCTION

Despite the introduction of the shakedown theorem by Melan in 1938 [2-3], intense research efforts started in the mid-sixties with a major focus to determine shakedown domains for pressure vessels [4], nuclear reactor components [5], and aeronautical applications [6]. Iterative elastic techniques have been proposed to obtain rapid and approximate bounds for limit and shakedown loads. The Iterative elastic techniques begin with an initial elastic solution which is modified in an iterative manner, through a series of linear elastic FE solutions, to redistribute stresses within the structure by changing the elastic moduli of the elements. The iterations proceed until a stress distribution in equilibrium with the externally applied load is reached. The iterative elastic techniques include the Elastic Compensation Method (ECM) introduced by Marriott [7], the Dhalla Reduction Procedure proposed by Dhalla [8] and the GLOSS R-Node method proposed by Seshadri [9]. The ECM is the most commonly used iterative elastic technique for shakedown load applications.

The problem of the large square plate with a small central hole has enjoyed wide attention by several researchers due to the stress concentration existing at the hole. Timoshenko and Goodier [10] reported stress function solution of the problem within the linear elastic domain. Hodge [11] presented analytical solution of the problem under monotonic equibiaxial tension for a material obeying linear hardening behavior. Chakrabarty [12] extended Hodge's analysis [11] and provided analytical solution of the problem for a nonlinear hardening material model under the same loading conditions. Belytschko [13] evaluated the limit load domain and certain magnitudes for the shakedown load of the same problem utilizing the FE method coupled with numerical optimization. Later Corradi and Zavelani [14] evaluated the shakedown domain using the FE method and linear programming techniques. The results of Belytschko [13] and Corradi and Zavelani [14] showed lack of accuracy which is mainly attributed to the small number of implemented elements due to the computing power restrictions at this early time (1972 and 1974) of FE development.

Stein et al. [15] developed an FE code and generated the shakedown domain for the same plate problem employing an EPP material. Later Stein and Huang [16] analytically determined the shakedown domain of the same problem coupled with optimization techniques employing a linear KH material. The results of Stein et al. [15] and Stein and Huang [16] were difficult to interpret since at the specific loading condition of equibiaxial tension, the shakedown load lied on the elastic domain where plasticity was not yet initiated. Reasons behind the illogical results of Stein et al. [15] and Stein and Huang [16] were investigated by Attia et al. [17] who presented a complete corrected solution. Furthermore, Attia et al. [17]

generated the shakedown domain of the plate employing the ECM and full elastic plastic cyclic loading FE simulations. Muscat et al. [18] analyzed the same problem and their solution agreed well with that of Attia et al. [17].

## PROBLEM DESCRIPTION

Figure 1(a) shows a schematic diagram of the square plate with a small central hole subjected to a system of uniform horizontal and vertical tensile stresses, ( $P_1$ ), and ( $P_2$ ) respectively. The horizontal and vertical stresses, ( $P_1$ ) and ( $P_2$ ), are assumed to vary cyclically in-phase between zero and a maximum magnitude,  $\bar{P}$ , as shown in Fig. 1(b). In order to generate the shakedown domain, the problem is solved for different values of ( $P_2/P_1$ ) ranging from 0 till 1 in increments of 0.1 (i.e. 0, 0.1, 0.2 ..... 0.9, 1) respectively.

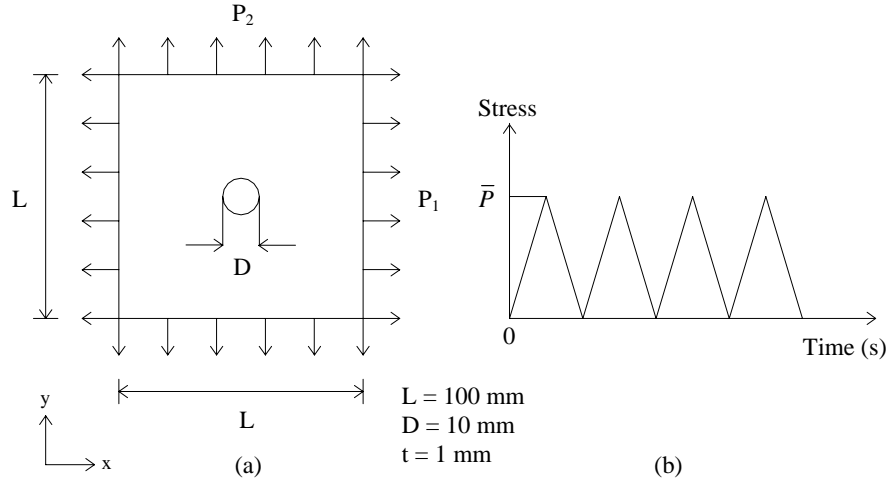


Figure 1: (a) Square plate with a small central hole - (b) Cyclic loading scheme on plate

## THE SIMPLIFIED TECHNIQUE

The simplified technique utilizes small displacement formulation and employs an elastic-linear strain hardening material model obeying the KH rule. The EPP material model is a special case of the elastic-linear strain hardening model but with minor modifications. Two FE analyses are performed. The first is an elastic analysis in which the cyclic loads ( $P_1$ ) and ( $P_2$ ), named the reference loads ( $P_{1-ref}$  and  $P_{2-ref}$ ), are monotonically applied and elastically deform the plate. The second analysis is an elastic-plastic analysis in which the cyclic loads ( $P_1$ ) and ( $P_2$ ) are applied in an increasing ramp pattern causing the strains within parts of the plate to exceed the material initial yield strain ( $\epsilon_0$ ).

The residual stress ( $\sigma_r$ ), scaled to the applied load increment ( $P_{1i}$  or  $P_{2i}$ ), is calculated according to Eq. (1) or Eq. (2) by subtracting the elastic stress ( $\sigma_E$ ) components (representing unloading) from the elastic-plastic stress ( $\sigma_{ELPL}$ ) components (representing loading) at every solution increment ( $i$ ). It is important to mention that the elastic ( $\sigma_E$ ) and the elastic-plastic ( $\sigma_{ELPL}$ ) stress components are output at the integration points of all the elements meshing the plate.

$$\sigma_{r_i} = \sigma_{ELPL_i} - \sigma_E \frac{P_{1i}}{P_{1-ref}} \quad (1) \quad , \quad \sigma_{r_i} = \sigma_{ELPL_i} - \sigma_E \frac{P_{2i}}{P_{2-ref}} \quad (2)$$

Therefore, a residual stress corresponding to every stress component is calculated. Then, an equivalent residual stress is calculated using the von Mises yield function. Since KH involves translation of the yield surface preserving its initial size, the corresponding yield criterion should be a function of both the state of stress and the coordinates of the yield surface current center. Hence, the equivalent residual stress ( $\sigma_{req}$ ) is expressed as follows:

$$\sigma_{req} = \frac{1}{\sqrt{2}} \left\{ \left[ \left[ (\sigma_{r_x} - \alpha_x) - (\sigma_{r_y} - \alpha_y) \right]^2 + \left[ (\sigma_{r_y} - \alpha_y) - (\sigma_{r_z} - \alpha_z) \right]^2 + \left[ (\sigma_{r_z} - \alpha_z) - (\sigma_{r_x} - \alpha_x) \right]^2 + \right. \right. \\ \left. \left. 6 \left[ (\tau_{r_{xy}} - \alpha_{xy})^2 + (\tau_{r_{yz}} - \alpha_{yz})^2 + (\tau_{r_{zx}} - \alpha_{zx})^2 \right] \right] \right\}^{\frac{1}{2}} \quad (3)$$

The terms  $\sigma_{r_x}$ ,  $\sigma_{r_y}$ ,  $\sigma_{r_z}$ ,  $\tau_{r_{xy}}$ ,  $\tau_{r_{yz}}$ , and  $\tau_{r_{zx}}$  are the residual stress components calculated using either Eq. (1) or Eq. (2). The terms  $\alpha_x$ ,  $\alpha_y$ ,  $\alpha_z$ ,  $\alpha_{xy}$ ,  $\alpha_{yz}$ , and  $\alpha_{zx}$  are the back stress components, determined from the KH shift tensor, responsible for the translation of the yield surface. For the EPP material, all the back stress components are set to zero and Eq. (3) reduces to following form:

$$\sigma_{req} = \frac{1}{\sqrt{2}} \left[ (\sigma_{r_x} - \sigma_{r_y})^2 + (\sigma_{r_y} - \sigma_{r_z})^2 + (\sigma_{r_z} - \sigma_{r_x})^2 + 6(\tau_{r_{xy}}^2 + \tau_{r_{yz}}^2 + \tau_{r_{zx}}^2) \right]^{\frac{1}{2}} \quad (4)$$

A computer program is developed to read the output of the elastic and the elastic-plastic analyses and calculate the residual stress components using Eq. (1) or Eq. (2) for all the integration points of all the elements meshing the plate at every elastic-plastic solution increment. The program then calculates equivalent residual stresses for all the integration points of all elements meshing the plate using Eq. (3) for a kinematically hardening material or Eq. (4) for an EPP material. The program then searches for the **minimum** load increment ( $P_{1i}$  or  $P_{2i}$ ) at which its corresponding calculated equivalent residual stress ( $\sigma_{req}$ ) slightly exceeds the material initial yield strength ( $Y_0$ ). Therefore, the preceding load increment ( $P_{1(i-1)}$  or  $P_{2(i-1)}$ ) is the shakedown limit load of the plate since its corresponding calculated equivalent residual stress ( $\sigma_{req}$ ) is either equal to or slightly less than the material initial yield strength ( $Y_0$ ). Hence, the load combination ( $P_{1(i-1)}$  and  $P_{2(i-1)}$ ) is the shakedown limit load of the plate for a given ( $P_2/P_1$ ) value.

The program outputs a list of elements with their corresponding integration points at which their calculated equivalent residual stresses ( $\sigma_{req}$ ) are either equal to or slightly less than the material initial yield strength ( $Y_0$ ). These integration points are the most critical points in the plate since they control its shakedown behavior. Exceeding the shakedown limit load, these critical points experience reversed plasticity or ratchetting behaviors depending on the plate loading conditions. The elastic limit load is determined through the elastic-plastic analysis (representing loading) by searching for the load increment corresponding to the first integration point(s) that experiences yielding.

In order to gain confidence in the simplified technique, full elastic-plastic cyclic loading FE simulations are performed using the output shakedown limit load combination ( $P_{1(i-1)}$  and  $P_{2(i-1)}$ , i.e.  $\bar{P}_{(i-1)}$ ) to check for shakedown behavior of the plate for both the KH and the EPP materials. Moreover, full elastic-plastic cyclic loading simulations are also performed but using the load combination increment ( $P_{1i}$  and  $P_{2i}$ ) just exceeding the output shakedown limit loads to check for reversed plasticity or ratchetting behaviors of the plate. The full cyclic loading simulations employ the cyclic loading pattern shown in Fig. 1(b).

## FINITE ELEMENT MODELING

Due to the presence of both geometric and applied loading symmetry about the x- and y- axes, only one quarter of the plate geometry is considered for the FE modeling. Figure 2(a) shows a schematic of the plate quarter model, boundary conditions, and the associated applied loading. The general purpose non-linear FE code ABAQUS/Standard [19] is used in analyzing the problem. Since the plate thickness is very small compared to the in-plane dimensions, plane stress four noded elements (CPS4) are used to mesh quarter the plate geometric model shown in Fig. 2(a). Since plane stress elements are used, the  $\sigma_{r_z}$ ,  $\tau_{r_{yz}}$  and,  $\tau_{r_{zx}}$  terms will commonly vanish from Eq. (3) and Eq. (4). In addition, the  $\alpha_z$ ,  $\alpha_{yz}$ , and  $\alpha_{zx}$  terms will vanish from Eq. (3). The nodes lying along the sides DE and AB, Fig. 2(a), are constrained in the x- and y- directions respectively, thereby preventing plate rigid body motion. Uniform horizontal and vertical tensile stresses,  $P_1$  and  $P_2$  respectively are applied as shown in Fig. 2(a). Upon conducting several mesh convergence checks, it was found that meshing quarter the plate geometry with 3200 plane stress elements provides adequate results. Care has been taken in order to ensure sufficiently small element size at the vicinity of the hole edge due to the existence of stress concentration at this region. Figure 2(b) shows the employed FE mesh of the plate quarter geometry. The plate material is assumed to be homogenous, isotropic, and made of steel having the following properties:  $E = 210 \text{ GPa}$ ,  $E_t = 0.05E$  (10500 MPa),  $\nu = 0.3$ , and  $Y_0 = 210 \text{ MPa}$ . Concerning the EPP material, the tangent modulus ( $E_t$ ) is set to zero.

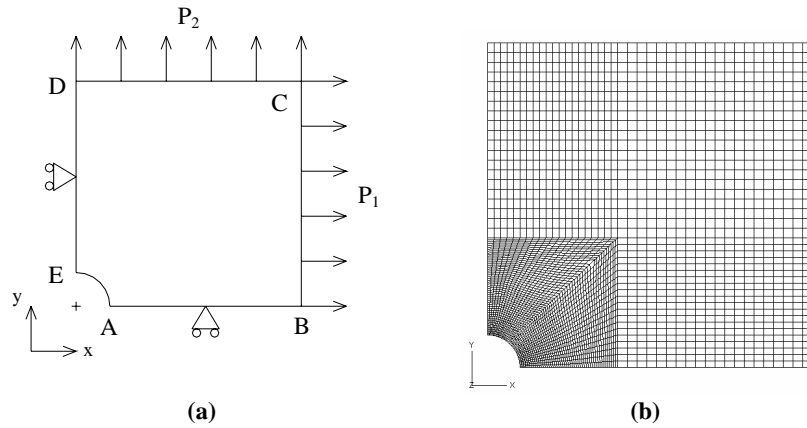


Figure 2: (a) Employed quarter plate geometry, boundary conditions, and applied loads – (b) Employed FE mesh on the plate quarter geometry

RESULTS AND DISCUSSION

Figure 3 shows the shakedown domain of the plate problem generated using the simplified technique. The output shakedown limit loads are normalized by the material initial yield strength ( $Y_0$ ). Imposed on Fig. 3 are the respective normalized limit load (maximum load carrying capacity under monotonic loading conditions) for the EPP material and the normalized elastic limit load forming the elastic region.

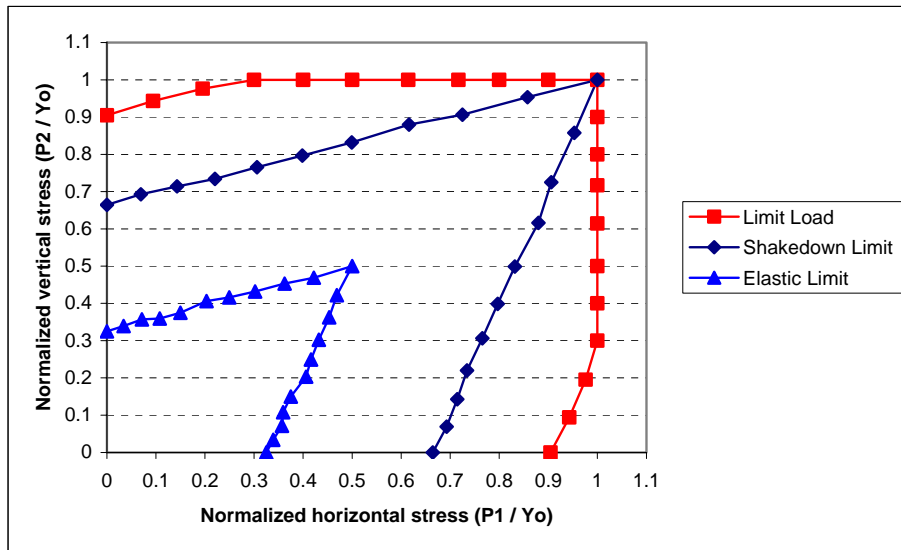
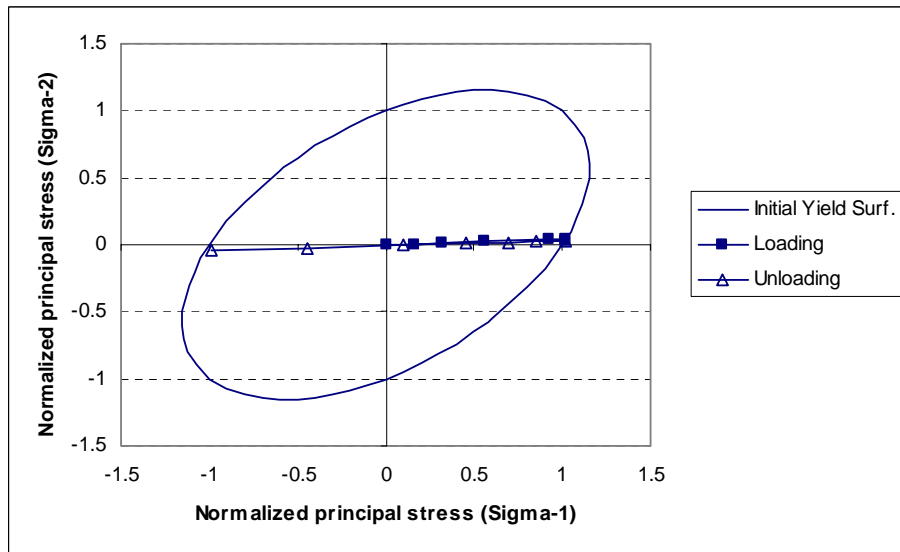


Figure 3: Limit load, Shakedown limit load, and elastic limit load domains of the plate with a small central hole under cyclic biaxial tension loading

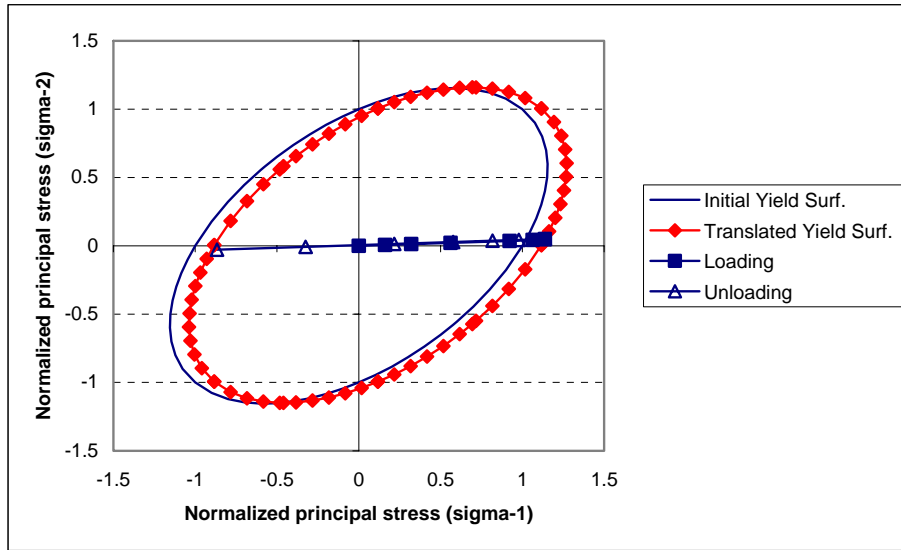
Inspection of detailed results of the simplified technique showed that the generated shakedown domain, shown in Fig. 3, is the same for both employed material models namely: the elastic-linear strain hardening material obeying the KH

rule and the EPP material. The reason behind this outcome is investigated through plotting the normalized principal stresses of the output critical integration points in the plate inscribed within their yield surfaces showing the loading and unloading paths under full cyclic loading using the shakedown limit load output by the simplified technique. Figure 4 shows the loading-unloading path of a critical integration point, output by the simplified technique employing the EPP material, under full cyclic loading for the ( $P_2/P_1 = 0.5$ ) case inscribed within its yield surface. The output critical integration point lies close to the hole circumference within the element at point (E) shown in Fig. 2(a). It could be noticed from Fig. 4 that the inscribed loading-unloading path almost represents uniaxial loading at the output integration point of concern. This loading pattern is expected since the hole circumference is a free edge and hence no radial component of stress exists and the element at point (E) experiences only the circumferential component of stress.

Figure 5 shows the loading-unloading path inscribed within the translated yield surface of the same integration point (output by the simplified technique) for the ( $P_2/P_1 = 0.5$ ) case employing the elastic-linear strain hardening material obeying the KH rule. Despite translation of the initial yield surface as a result of KH, shown in Fig. 5, the maximum change in stresses along the unloading path is almost equal to the maximum change in stresses along the unloading path inscribed within the fixed yield surface shown in Fig. 4 for the same ( $P_2/P_1 = 0.5$ ) case employing the EPP material. This explains the equal shakedown limit loads resulting from the KH and the EPP material behaviors for all the values of ( $P_2/P_1$ ) ranging from 0 till 1.

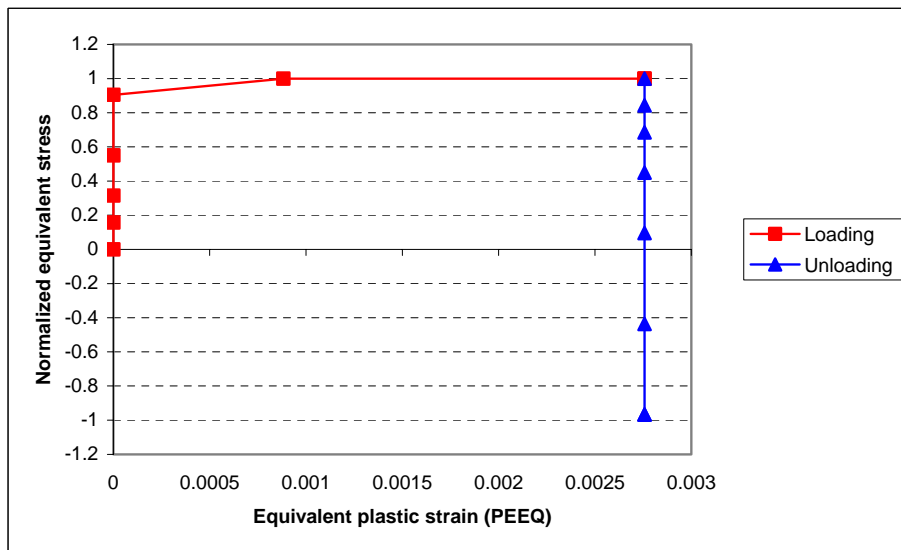


**Figure 4: The loading-unloading path of the ( $P_2 / P_1 = 0.5$ ) case inscribed within the yield surface of the output critical integration point**



**Figure 5: Loading-unloading path of the ( $P_2 / P_1 = 0.5$ ) case inscribed within the translated yield surface for the plate employing the elastic-linear strain hardening material obeying the KH rule**

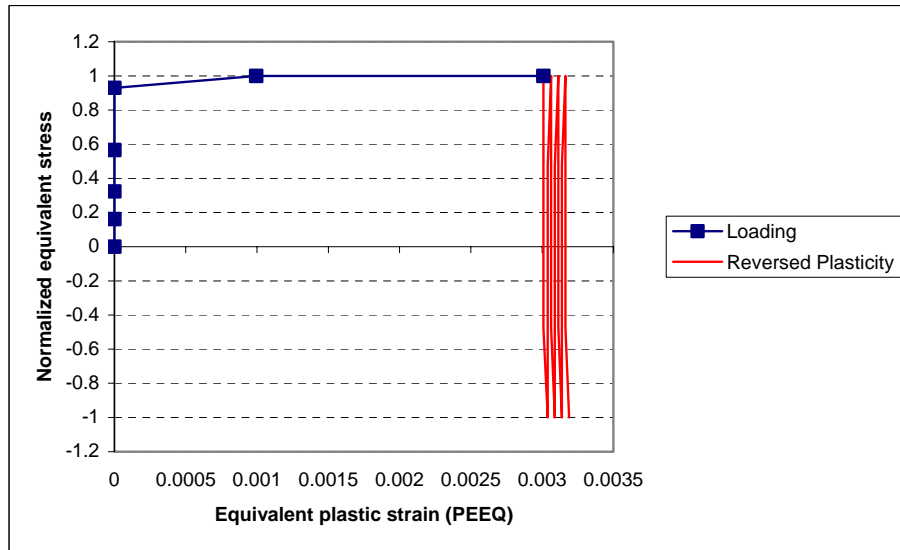
In order to gain confidence in the simplified technique, full elastic-plastic cyclic loading FE simulations are conducted using the shakedown limit loads output by the simplified technique following the cyclic loading pattern shown in Fig. 1(b). The full cyclic loading of the ( $P_2/P_1 = 0.5$ ) case employing the elastic-linear strain hardening and the EPP material models is used as a representative sample of the ( $P_2/P_1$ ) values ranging from 0 till 1. The shakedown behavior is illustrated by plotting the normalized equivalent stress [(von-Mises stress) / ( $Y_0$ )] versus the equivalent plastic strain (PEEQ) as shown in Fig. 6 for the ( $P_2/P_1 = 0.5$ ) case (at one of the critical integration points output by the simplified technique) employing the EPP material.



**Figure 6: Shakedown behavior of the ( $P_2 / P_1 = 0.5$ ) case (employing the EPP material model) under full cyclic loading using the shakedown limit load output by the simplified technique**

The (+1) value on the normalized equivalent stress axis, Fig. 6, denotes yielding in tension while the (-1) value on the same axis denotes yielding in compression. The solid square legend, shown in Fig. 6, represents the loading phase of the first load cycle of Fig. 1(b) which plastically strains the output critical integration point till reaching a maximum PEEQ value of 0.00276 while maintaining a maximum constant normalized equivalent stress of (+1) as a result of employing the EPP material. The solid triangle legend represents the unloading phase of the first cycle of Fig. 1(b) and the loading and unloading phases of the subsequent cycles. Hence, the shakedown behavior is characterized by a pure elastic response represented by the vertical straight line with triangle legend, shown in Fig. 6, along which unloading of the first cycle and the subsequent loadings and unloadings occur at a constant PEEQ resulting from the loading phase of the first load cycle. The negative normalized equivalent stresses, shown in Fig. 6, are assigned to account for compressive states of stress by checking the sign of the mean stress at every solution increment in the full cyclic loading analysis. A negative mean stress signifies compression of the plate material; hence, a negative sign is assigned to the corresponding normalized equivalent stress. In Fig. 6, the minimum normalized equivalent stress reached at unloading recorded a value of (-0.97); therefore, the maximum difference between the loading and the unloading phases recorded a normalized stress value of (+1.97) [i.e.  $+1 - (-0.97) = +1.97$ ] which is slightly less than (+2). The (+2) value signifies  $(2Y_0)$  representing the constant size of the fixed yield surface, Fig. 4, and the maximum permissible residual stress to be reached by any integration point within the plate at unloading beyond which the shakedown behavior is violated.

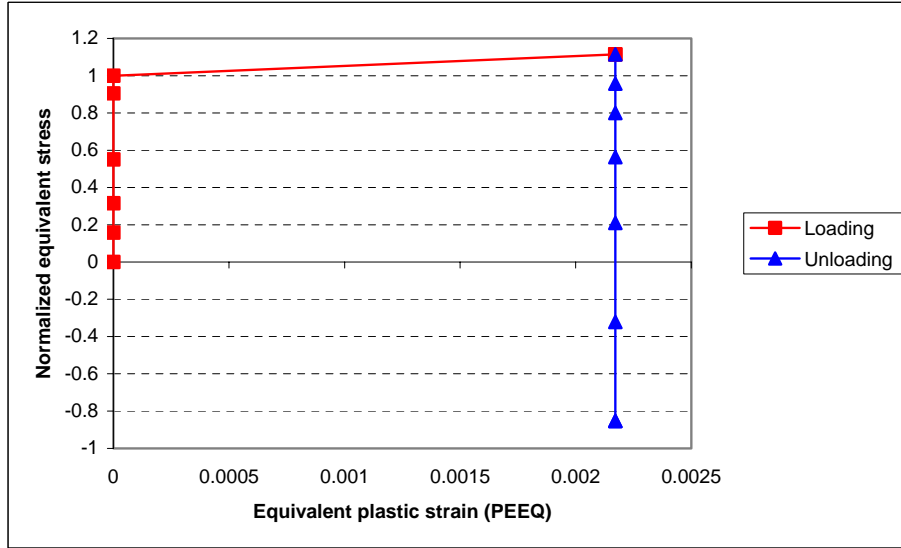
The output critical integration point of the  $(P_2/P_1 = 0.5)$  case experiences reversed plasticity behavior upon cyclically loading the plate with the load combination increment  $(P_{1i}$  and  $P_{2i})$  just exceeding the output shakedown limit load combination,  $(P_{1(i-1)}$  and  $P_{2(i-1)})$ . Figure 7 shows reversed plasticity behavior of the output critical integration point for the  $(P_2/P_1 = 0.5)$  case upon cyclically loading the plate with the load combination increment  $(P_{1i}$  and  $P_{2i})$ . It could be noticed that the critical integration point experiences yielding in tension, (+1), at loading and yielding in compression, (-1), at unloading at every cycle of Fig. 1(b).



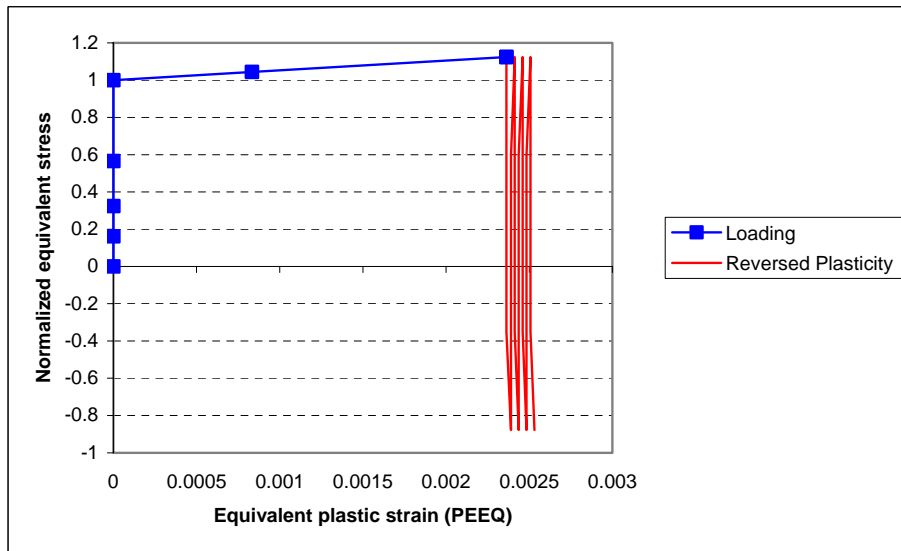
**Figure 7: Reversed plasticity behavior of the  $(P_2 / P_1 = 0.5)$  case (employing the EPP material model) under full cyclic loading upon exceeding the shakedown limit load output by the simplified technique**

Figure 8 shows the shakedown behavior of one of the critical integration points output by the simplified technique for the  $(P_2/P_1 = 0.5)$  case employing the elastic-linear strain hardening material obeying the KH rule. Unlike the loading phase shown in Fig. 6 for the  $(P_2/P_1 = 0.5)$  case employing the EPP material, the loading phase of Fig. 8 is characterized by a long sloped line starting at a normalized equivalent stress value of (+1) till a maximum recorded value of (+1.114). The long sloped line represents the hardening experienced by the material of the critical integration point during loading which ultimately leads to translation of the point's yield surface, as shown in Fig. 5, preserving its initial size since the KH rule is obeyed. In Fig. 8, the minimum normalized equivalent stress reached at unloading recorded a value of (-0.853); therefore, the maximum difference between the loading and the unloading phases recorded a normalized stress value of (+1.967) [i.e.  $+1.114 - (-0.853) = +1.967$ ] which is slightly less than (+2) denoting shakedown behavior under KH behavior.

The critical integration point of the ( $P_2/P_1 = 0.5$ ) case experiences reversed plasticity behavior upon cyclically loading the plate with the load combination increment ( $P_{1i}$  and  $P_{2i}$ ) just exceeding the shakedown limit load combination ( $P_{1(i-1)}$  and  $P_{2(i-1)}$ ). Figure 9 shows reversed plasticity behavior of the critical integration point of the ( $P_2/P_1 = 0.5$ ) case upon cyclically loading the plate with the load combination increment ( $P_{1i}$  and  $P_{2i}$ ).



**Figure 8: Shakedown behavior of the ( $P_2 / P_1 = 0.5$ ) case (employing the elastic-linear strain hardening material obeying the KH rule) under full cyclic loading using the shakedown limit load output by the simplified technique**



**Figure 9: Reversed plasticity behavior of the ( $P_2 / P_1 = 0.5$ ) case (employing the elastic-linear strain hardening material obeying the KH rule) under full cyclic loading upon exceeding the shakedown limit load output by the simplified technique**

It was soon apparent for this problem that only reversed plasticity behavior occurs upon exceeding the shakedown domain shown in Fig. 3 for all the values of ( $P_2/P_1$ ) for both the KH and the EPP material models. Figure 10 shows a comparison between the shakedown domains of the large plate with a small central hole generated using different solutions.



The solutions include the presented simplified technique of concern, an analytical solution presented by Chakrabarty [12], a solution based on full elastic-plastic cyclic loading FE analyses presented by Attia et al. [17], and a solution based on applying the ECM by Attia et al. [17]. It could be noticed from Fig. 10 that the shakedown domain generated by the simplified technique is the closest and almost identical to the analytical solution presented by Chakrabarty [12]. The solution of the simplified technique is also very close to the full elastic-plastic cyclic loading solution presented by Attia et al. [17]. The ECM solution showed some differences from the other presented solutions since it performs a series of iterations to determine the shakedown limit load resulting in round-off errors which ultimately affects the solution accuracy.

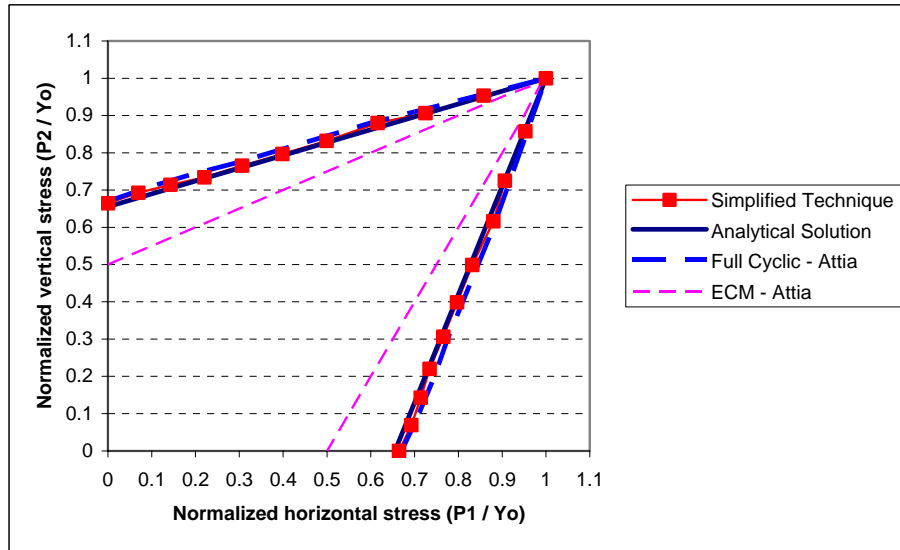


**Figure 10: Comparison between the shakedown domain generated by the simplified technique and other solutions presented in the literature**

## CONCLUSION

The simplified technique previously developed to determine the shakedown limit load for structures experiencing uniaxial states of stress is successfully developed to handle cyclic biaxial loading of a large plate with a small central hole employing two material models namely: an elastic-linear strain hardening material obeying the KH rule and an EPP material. The simplified technique is successfully applied to the problem of a large square plate with a small central hole subjected to cyclic biaxial tension along its edges. The outcomes of the simplified technique showed excellent correlation with the analytical solution of the plate problem presented by Chakrabarty [12] and the full elastic-plastic cyclic loading solution presented by Attia et al. [17].

Shakedown behavior is observed upon cyclically loading the plate with the shakedown limit loads output by the simplified technique. Reversed plasticity behavior is observed upon cyclically loading the plate with load magnitudes just exceeding the shakedown limit loads output by the simplified technique for all the  $(P_2/P_1)$  loading ratios. No ratchetting behavior is observed upon exceeding the shakedown domain of the plate. Hence, both the geometry and the cyclic loading nature of the present plate problem influence its post-shakedown behavior. It is also shown that material hardening had no effect on the shakedown limit load of this problem (in comparison to employing EPP material).

The computational time required by the simplified technique to generate the whole shakedown domain of the plate is totally insignificant compared to performing full elastic-plastic cyclic loading analyses. The full elastic-plastic cyclic loading analyses require an initial guess (load magnitude) followed by an iterative series of guesses (several cyclic loading iterations) until the shakedown limit load is determined forming a single point on the shakedown domain. In addition, thorough understanding of the loading nature and prior knowledge of the possible regions within the structure containing the critical points controlling its shakedown behavior are required. Contrarily, the simplified technique does not require any prior knowledge of the expected critical regions controlling the structure shakedown behavior since it automatically checks all points within the structure.

**ACKNOWLEDGMENTS**

The American University in Cairo is greatly acknowledged for use of its advanced computational facilities.

**NOMENCLATURE**

$D$	Hole diameter	$\nu$	Poisson's ratio
$E$	Young's modulus	$\sigma_E$	Elastic stress components
$E_t$	Tangent modulus	$\sigma_{ELPL}$	Elastic-plastic stress components
$L$	Length of plate edge	$\sigma_r$	Residual stress components
$i$	Elastic-plastic solution increment	$\varepsilon$	Strain
$t$	Plate thickness	$\varepsilon_0$	Material initial yield strain
$Y_0$	Material initial yield strength		
$\alpha$	Kinematic hardening back stress		

**REFERENCES**

- [1] Abdalla, H.F., Younan, M.Y.A., and Megahed, M.M., "A Simplified Technique for Shakedown Load Determination," Proc. Of the 18th International Conference on Structural Mechanics in Reactor Technology, pp 1315-1328, Beijing, China, August 2005.
- [2] Melan, E., "Der Spannungszustand eines Mises-Henckyschen Kontinuums bei veränderlicher Belastung," Sitzber. Akad. Wiss., Vol. 147, 1938, pp. 73-78.
- [3] Melan, E., "Zur Plastizität des räumlichen Kontinuums," Ing. Arch., Vol. 8, 1938, pp. 116-126.
- [4] Leckie, F.A. and Penny, R.K., "Shakedown Pressure for Radial Nozzles in Spherical Pressure Vessels," International Journal of Solids and Structures, Vol. 3, 1967, pp. 743-755.
- [5] Bree, J., "Elastic-Plastic Behaviour of Thin Tubes Subjected to Internal Pressure and Intermittent High Heat Fluxes with Application to Fast Nuclear Reactor Fuel Elements," Journal of Strain Analysis, Vol. 2, 1967, pp. 226-238.
- [6] Parkes, E.W., "Structural Effects of Repeated Thermal Loading," Thermal Stress, 1964, (Edited by Benham et al.), Pitman, London.
- [7] Marriott, D.L., "Evaluation of Deformation or Load Control of Stress under Inelastic Conditions Using Finite Elements Stress Analysis," Proc. Of the ASME PVP division conference, Vol. 136, 1988, pp. 3-9.
- [8] Dhalla, A.K., "A Simplified Procedure to Classify Stresses for Elevated Temperature Service," ASME transactions, PVP division conference, Vol. 120, 1987, pp. 177-188.
- [9] Seshadri, R., "The Generalized Local Stress Strain (GLOSS) Analysis-Theory and Applications," ASME Journal of Pressure Vessel Technology, Vol. 113, 1991, pp. 219-227.
- [10] Timoshenko, S.P. and Goodier, J., *Theory of Elasticity*, McGraw-Hill, New York, 1953.
- [11] Hodge Jr., P.G., "The Effect of Strain Hardening in an Annular Slab," Journal of Applied Mechanics, Vol. 20, 1953, pp. 530-536.
- [12] Chakrabarty, J., *Theory of Plasticity*, McGraw-Hill, 1987.
- [13] Belytschko, T., "Plane Stress Shakedown Analysis by Finite Elements," International Journal of Mechanical Sciences, Vol. 14, 1972, pp. 619-625.
- [14] Corradi, L. and Zavelani, I., "A Linear Programming Approach to Shakedown Analysis of Structures," Comp. Mech. Appl. Mech. Eng., Vol. 3, 1974, pp. 1-37.
- [15] Stein, E., Zhang, G., and König, J., "Shakedown with Nonlinear Strain-Hardening Including Structural Computation Using Finite Elements Method," International Journal of Plasticity, Vol. 8, 1992, pp. 1-31.
- [16] Stein, E. and Huang, Y., "An Analytical Method for Shakedown Problems with Linear Kinematic Hardening Materials," Int. J. Solids Structures, Vol. 31 No. 18, 1994, pp. 2433-2444.
- [17] Attia, M.S., Abdel-Karim, M., and Megahed, M.M., "Shakedown Analysis of an Infinite Plate with a Central Hole under Biaxial Tension," Proc. Of the 7th International Mechanical Design and Production Conference, Cairo, Egypt, February 2000.
- [18] Muscat, M., Mackenzie, D., and Hamilton, R., "Evaluating Shakedown under Proportional Loading by Non-linear Static Analysis," Comp. Struct., Vol. 81, 2003, pp. 1727-1737.
- [19] Hibbitt, Karlsson and Sorensen, Inc., ABAQUS/Standard User's Manual, Providence, R. I., 2006.